Aquaculture
December 2022, Volume 561 Pages 738683 (13p.)
https://doi.org/10.1016/j.aquaculture.2022.738683
https://archimer.ifremer.fr/doc/00788/89970/

The effects of experimental temperature increase on gametogenesis and heat stress parameters in oysters: Comparison of a temperate-introduced species (*Crassostrea gigas*) and a native tropical species (*Crassostrea corteziensis*)

Rodríguez-Jaramillo C. [1, 2], García-Corona Jose Luis [3], Zenteno-Savín T. [1], Palacios E. [1, *]

[1] Centro de Investigaciones Biológicas del Noroeste (CIBNOR), Instituto Politécnico Nacional 195, Col. Playa Palo de Santa Rita Sur, La Paz 23096, B.C.S, Mexico
[2] Universidad Autónoma de Baja California Sur, Ciencias Marinas y Costeras (CIMACO), Carretera al Sur Km. 5.5, La Paz 23080, B.C.S, Mexico
[3] Laboratoire des Sciences de l'Environnement Marin (LEMAR), Institut Universitaire Européen de la Mer, Université de Bretagne Occidentale, UMR 6539 CNRS/UBO/IRD/IFREMER, 29280 Plouzané, France

* Corresponding author : E. Palacios, email address : epalacio@cibnor.mx

Abstract :

The effect of thermal stress during reproduction was experimentally evaluated in the oyster Crassostrea gigas, a temperate species, and in the tropical oyster Crassostrea corteziensis. The temperature was gradually increased (1 °C day−1) from 20 °C to 34 °C for two weeks. As expected, C. gigas was the species most affected by heat stress, with the highest mortality rate ($P < 0.05$) starting at 28 °C, while mortality in C. corteziensis was significant only at 34 °C. The reproductive effort at higher temperatures was reflected in C. gigas as the highest index of mature oocytes and the largest rate of atresic and degenerated oocytes. C. corteziensis showed significant increases in the proliferation of early-developing oocytes at maximum temperatures. Lipid peroxidation and lipofuscin accumulation significantly increased in both species at maximum temperatures, with levels in C. gigas being 8-fold higher than in C. corteziensis. A significant loss of biomass and glycogen reserves stored in gonads was found in C. gigas at 34 °C. The mRNA signal of Hsp70 was detected in gonadic tissues from both oysters after thermal stress for in situ hybridization (ISH), with a temperature increase in both species; the cover area of Hsp70 was significantly higher in C. gigas during the experiment. Hemocyte infiltration significantly increased with increasing temperature in both oyster species, and apoptosis was strongly correlated with Hsp70 in both species ($r = 0.93$; $P < 0.05$). These results could explain the high tolerance that C. corteziensis has to thermal stress compared to C. gigas and could be used to adapt aquaculture strategies to the use of native species in subtropical climates to reduce summer mortality events.

Highlights

► Different mechanisms are triggered in temperate and subtropical oysters to withstand thermal stress. ► Histochemistry and *in situ* hybridization can pinpoint changes at cellular and tissue levels. ► *C. corteziensis* produce more *Hsp70* and apoptosis compared to *C. gigas* when temperature increases. ► *C. gigas* produce more lipofucsines, TBARS and degenerated oocytes when temperature increases.

Keywords : Summer mortality, Hemocyte apoptosis, Heat shock proteins, Lipid peroxidation, Atretic oocytes, Autophagy

1. Introduction

Oysters in the reproductive stage are acutely susceptible to thermal stress, particularly during the summer months, with up to 90% mortality for the Pacific oyster *Crassostrea gigas* reported in some countries (Samain et al., 2007; Fleury et al., 2020), an event commonly referred to as "summer mortality" (Soletchnik et al., 2006; Cotter et al., 2010; Huvet et al., 2010; Fleury et al., 2020). This mortality has been attributed to accelerated gonadal development and spawning that deplete energy (Berthelin et al., 2000; Delaporte et al., 2007; Samain et al., 2007). Continuous and drastic die-offs of temperate *C. gigas* have caused major economic losses around the globe (Huvet et al., 2010; Delisle et al., 2020; Fleury et al., 2020), which seriously threaten the food supply in growing areas and the viability of entire populations by failures in spat recruitment (Wendling et al., 2013). Summer mortalities are further enhanced in warm climates where *C. gigas* has been introduced and is the most important commercial species, even if it is outside its distribution range. There are, however, native species that are more tolerant to increased temperatures that are not used commercially, such as *Crassostrea corteziensis*, which is well adapted to semitropical waters and has been identified as a viable option for farmers due to its low mortality rates, fast growth, and continuous reproduction during warm seasons (Chávez-Villalba et al., 2007; Castillo-Durán et al., 2010; Rodríguez-Jaramillo et al., 2017).

Here, we endeavored to examine whether there exist differences in reproductive physiology that would make one species more tolerant to thermal shock in comparison to the other. Most reproductive studies have focused on *C. gigas*, where it has been described that when there are adverse environmental conditions that can produce physiological stress, the gonad presents hemocyte infiltration and phagocytosis of surrounding material (Le Pennec et al.,

1991; Dutertre et al., 2009; Huvet et al., 2010; Rahman et al., 2019) and even apoptosis (Lang et al., 2009; Sokolova et al., 2009; Kiss, 2010; Wang et al., 2018; Delisle et al., 2020). Prespawning oocyte autolysis, or atresia, appears to be part of an intricate and organized pathway employed by oysters during simultaneous intense reproductive effort and detrimental conditions (Beninger et al., 2017), which might allow oysters to divert part of the energy that was previously invested in unsustainable gametogenesis. The high metabolic rates necessary to support gametogenesis and environmental stress simultaneously lead to the accumulation of oxidative damage (Abele et al., 2007; Guerra et al., 2012), characterized by the progressive oxidation of lipids and lipoproteins and the subsequent accumulation of the fluorescent aging pigment lipofuscin (Keller et al., 2004). Products of oxidative damage can compromise cellular function and maintenance in bivalves (Abele et al., 2007; Guerra et al., 2012) and could be implicated in apoptosis and the induction of autophagy (Terahara & Takahashi, 2008; Eisenberg-Lerner et al., 2009). Evidence suggests that thermal stress has strong nonlethal effects on the "heat shock response" by means of the expression of proteins from the *Hsp*70 family, which are capable of acting as molecular chaperones and inducing thermotolerance in *Crassostrea spp.* against nonlethal temperatures but above the physiological optimal range (Lang et al., 2009; Jackson et al., 2011; Hurtado-Oliva et al., 2015). Although temperature strongly drives summer mortality events in oysters (Samain et al., 2007; Delisle et al., 2020; Fleury et al., 2020), no studies have assessed the compensatory capabilities and effects of thermal stress during reproduction in oyster species with different ranges of native-distribution that are farmed in the same geographical area. To test the question outlined above, a bioassay of adult oysters of the two species was carried out under controlled laboratory conditions during which the water temperature was increased from 20 °C to 34 °C (1 °C per day). The

94 main objective of this study was to evaluate the effect of the experimental increase in
95 temperature on the overall physiological responses of both *C. gigas* and *C. corteziensis*
96 during gametogenesis.
97
98 **2. Materials and methods**
99 **2.1. Source and management of oysters**
100 Diploid adult oysters were produced and cultured in controlled conditions in a
101 commercial system in Topolobampo, Sinaloa, México. A total of 70 adults of *C. gigas*
102 (length = 12.7 ± 0.2 cm) and 70 of *C. corteziensis* (length = 10.2 ± 0.1 cm) were
103 collected, packed in ice, and transported by plane to the aquaculture experimental
104 facilities of the Universidad Autónoma de Baja California Sur (UABCS) in La Paz, Baja
105 California Sur, México. On arrival, oysters were washed and scrubbed to eliminate
106 epibionts. Histological inspection at the start of the experiment using 10 oysters of each
107 species showed that the animals were in good health and in early gametogenesis (stage
108 I) according to Rodríguez-Jaramillo et al. (2008).
109
110 **2.2. Experimental design and increasing temperature**
111 The oysters were separated by species (60 adults of *C. gigas* and 60 adults of *C.*
112 *corteziensis*) and placed in six 100 L tanks (20 oysters per tank) supplied with filtered
113 seawater (1 μm filtered and UV-treated aerated; 20 ± 1 °C, pH 8.3 ± 0.1, and 35.1 ± 0.1
114 PSU). Animals were fed a daily ratio of an algal mixture of *Chaetoceros gracilis*, *C.*
115 *calcitrans* and *Isochrysis galbana* (50:25:25 equivalent volume) at a density of 4^{10} cells
116 $oyster^{-1}$ day^{-1} throughout the whole experiment. After 20 days of acclimatization, the
117 temperature was increased 1 °C day^{-1} in two of the three tanks of each species using

118 submersible electric heaters (± 1 °C) until reaching 34 °C after 2 weeks. The third tank
119 housing each species remained at 20 ± 1 °C as a control.
120 Sequential oyster samplings were performed at the beginning of the experiment (20 ±
121 1 °C), after one day (22 ± 1 °C), after 6 days (at 28 ± 1 °C), and after 12 days (at 34 ±
122 1 °C); 15 animals per tank (including controls) were sampled at each time. During each
123 sampling, biometric variables of wet weight (flesh without shell) and size (shell total
124 length) were recorded. The survival of the organisms was assessed daily.
125
126 **2.3. Quantitative histology and histochemistry**
127 Cross-sections of the mid-visceral mass (~3 mm) from each oyster were fixed in Davidson,
128 paraformaldehyde in phosphate-buffered saline (PBS), and Karnovsky solutions processed
129 and embedded in paraffin (Paraplast X-Tra, Mc Cormick Scientific, San Diego, CA, USA)
130 and resin (JB-4 plus Polyscience Inc, Warrington, PA), respectively, according to
131 Rodríguez-Jaramillo et al. (2008). Paraffin 4-µm thick tissue sections were stained with
132 hematoxylin-eosin to analyze the general morphology of the gonads, Periodic Acid-Schiff
133 (PAS) for neutral carbohydrates (in magenta color), Sudan Black B (SBB) to detect neutral
134 and polar lipids in black-bluish and gray hues, respectively, and Kinyoun Carbol Fuchsin
135 (KCF) for demonstration of reddish-brown lipofuscin-like inclusions (Rodríguez-Jaramillo
136 et al., 2008). Polychromatic staining was used in semi-fine (0.5 µm) resin cuts to analyze
137 the gonad cellular structure and to compare the tissue and morphological characteristics of
138 the oysters (Rodríguez-Jaramillo et al., 2008).
139 The histological slides were digitalized at high resolution (600 dpi; 20×), and three
140 randomly selected images were processed with Image-Pro Premier v.9.0 software (Media
141 Cybernetics, Silver Spring, MD, USA). The software relies on automatic calculations of the

142 area (μm^2) occupied by tissues, cells, carbohydrates, and lipids based on the segmentation
143 of pixels in the image in relation to the intensity of the specific color of each cell type,
144 tissue, or biochemical component according to each staining technique mentioned above.
145 The gonad coverage area (GCA), connective tissue index (CTI), oocyte index (OI),
146 hemocyte index (HI), carbohydrate index (CHI), and lipid index (LI) were also determined.
147 The calculations of each index (τ_{index})were based on those described by Rodríguez-
148 Jaramillo et al. (2008) using the formula:

149 $$\tau_{index} = \frac{\tau}{\beta} * 100$$

150 where τ represents the coverage area of each specific tissue, cell, or component, and β is
151 the total area of the image.
152 The gonad sections stained with the lipophilic dye KCF were digitalized and analyzed as
153 described above. The lipofuscin area was not expressed as an index but as μm^2 because
154 the distribution of the pigment granules was not homogeneous within the tissues.
155 The developmental stages used to classify the male and female gametes of both oyster
156 species were based on those described by Rodríguez-Jaramillo et al. (2008). The frequency
157 of each oocyte type (oogonia, previtellogenic, vitellogenic, postvitellogenic, and atretic
158 oocytes) as well as spermatogonia, spermatocytes, and spermatozoa was determined by
159 means of digital image analysis (Image-Pro Premiere) within a predetermined area of 1.44
160 m^2 at 20× in the same three sections where the gonad coverage area was calculated to
161 estimate the proportion of each area occupied by each gamete type.
162 For the oocytes in particular, additional features were estimated as indicators of the impact
163 of thermal shock on oyster reproduction. The area (A) of ~50 oocytes per female was
164 determined using digitalized images taken at 40× from three different regions of the ovary.

Oogonia analysis was performed at 100×. The images were processed with SigmaScan software (Systat Software, Inc., San Jose, CA, USA) to calculate the theoretical diameter (TD) of oocytes using the formula proposed by Saout *et al*. (1999):

$$DT = \sqrt{4A/\pi}$$

2.4. Lipid peroxidation

The levels of lipid peroxidation were measured in the gonads from each oyster by quantifying the content of thiobarbituric acid reactive substances (TBARS). Frozen (-80 °C) samples were homogenized in cold phosphate buffer solution (50 mM, pH 7.5) and phenyl-methyl-sulfonyl-fluoride solution, and 250 µL of the supernatant extracts were incubated for 15 min at 37 °C and then cooled to 4 °C for 15 min. The reaction was stopped by adding a mix of 12.5% trichloroacetic acid and 0.8 mol mL^{-1} hydrochloric acid, followed by 1% TBA. The extracts were stirred in an ice water bath, incubated for 10 min at 90 °C, cooled to room temperature, and centrifuged at 1509 x *g* for 10 min at 4 °C. The supernatants were recovered, placed in 200 µL microplate wells in triplicate, and read at 560 nm. The TBARS content was quantified using a standard curve (0–10 pmoles mL^{-1}) using 10 µmol mL^{-1} 1,1,3,3-tetraethoxypropane. The total protein concentration per tissue was analyzed using the method of Bradford (1976), which uses a commercial colorimetric reagent (B6916, Sigma-Aldrich, St. Louis, MO) and bovine serum albumin (9048-46. -8, Sigma-Aldrich) as a standard. The analysis was performed in triplicate in a microplate reader at 620 nm, and the results were reported as mg mL^{-1} of protein. The TBARS concentration was expressed as nmol TBARS mg^{-1} protein (Guerra et al., 2012).

2.5. *Hsp70* cDNA partial cloning

For RACE-PCR amplification of *Hsp70* mRNA ends of both species, gene-specific primers (GenBank AF144646.1; sense 5'-GCA AGT AAA CCC ATG ATC AAA-3' Tm 63.14 °C; antisense: 5'-GAG ACA TCA AAG GTT CCT CCT-3' Tm 61.28 °C) were designed using highly conserved regions of the *Hsp70* transcript in *C. gigas*. The amplification efficiency of primers was tested by PCR in samples of *C. gigas* and *C. corteziensis*. Subsequently, 12.5 µL of PCR was prepared containing 2 µL of cDNA, 0.48 µM of each primer, 0.2 µM dNTP mix (Invitrogen), 2.5 mM $MgCl_2$, 1X PCR buffer, and 0.2 U of Platinum *Taq* DNA polymerase (Invitrogen). The amplification conditions were the same as those described by Fabioux et al. (2005). PCR products (400–500 bp) were separated using electrophoresis, and fragments were gel-excised, purified using the QIAquick Gel Extraction Kit (Cat No. 28706X4 Qiagen, Venlo, Netherlands), subcloned into the plasmid vector P Gem (Invitrogen), transformed into *Escherichia coli* competent cells (Invitrogen), and sequenced (GENEWIZ, San Diego, CA, USA).

2.6. *In situ* hybridization and apoptotic cell death

The *Hsp70* transcripts were localized in gonad and digestive gland tissues from *C. gigas* and *C. corteziensis* through *in situ* hybridization (ISH). Sense and antisense single-stranded *Hsp70* DNA probes were prepared by random-priming PCR and tagging them with the DIG-DNA Labeling and Detection Kit® (Cat. No. 11093657910 Roche Applied Science, Penzberg, Germany). The template was the *in vitro* linearized plasmid *Hsp70* DNA fragment from *C. gigas* and *C. corteziensis*. Cross-sections (~ 0.5 g) from each oyster were stored in 4% paraformaldehyde for 48 h, dehydrated in an ethanol series

213 (70–100%) prepared with DEPC-treated water (Invitrogen), and embedded in paraffin
214 (Rodríguez-Jaramillo et al., 2008). Thin sections (4 µm) were mounted on poly-L-
215 lysine-coated glass slides (Sigma-Aldrich, St. Louis, MO, USA) under RNase-free
216 conditions. Rehydrated sections were permeated for 15 min with 10 µg mL^{-1} proteinase
217 K (Sigma-Aldrich). The tissue hybridization procedure was performed as described by
218 Boullot et al. (2017) using 5 µL of each DNA probe and anti-DIG antibody coupled
219 with alkaline phosphatase (Roche) at a 1:500 dilution. Hybridization without probes
220 was used as a negative control. Slides were mounted and digitalized at 20×.
221 Additionally, an *in situ* Cell Death Detection Kit® (Cat. No. 11684795910 Roche
222 Applied Science, Mannheim, Germany) was used following the provider's instructions
223 to find fragmented DNA strands in apoptotic cells using a fluorescent marker for
224 terminal deoxynucleotidyl transferase (TdT) dUTP nick-end labeling (TUNEL). For
225 both the ISH and TUNEL probes, an image signal processing technique (Rodríguez-
226 Jaramillo et al., 2008) was applied using Image-Pro Premiere software for the automatic
227 identification of color pixels expressed as area (μm^2).
228
229 **2.7. Statistical analysis**
230 *A priori* Shapiro-Wilk and Bartlett's tests were applied to confirm the normal frequency
231 distribution and homogeneity of variances of the data. Bifactorial analyses (factors: Species
232 and Temperature) of variance (ANOVA) were used to evaluate the effect of thermal shock
233 in the two species of oysters. An angular transformation was applied to the values
234 expressed in percentages before analysis, but data are reported untransformed as the mean ±
235 standard error. In cases where significant differences were found, a Tukey test (HSD) *post*
236 *hoc* analysis of means comparison was used. A Pearson correlation coefficient was run to

establish the relationship between temperature increase and oocytes with distended endoplasmic reticulum or vacuolated oocytes, hemocyte infiltration, and hemocytes in apoptosis of both species of oysters. Another correlation was made between the carbohydrate coverage area and the sum of degenerating oocytes. Differences were considered statistically significant at $P < 0.05$ for all analyses (Zar, 2010). All analyses were performed using Statistica software 8.0 (StatSoft Inc., Tulsa, UK).

2. RESULTS

3.1. Oyster survival and biometrics

Survival was significantly affected by species, temperature, and their interaction. For *C. gigas*, survival decreased ($P < 0.05$) with increasing temperature, with the lowest survival rate at 34 °C. For *C. corteziensis,* significant decreases in survival were found only at 34 °C. After two weeks of thermal stress, the survival rate for *C. gigas* was 91% and was 97% for *C. corteziensis* (Fig. 1A).

Total length was different only between the species, with *C. gigas* being larger than *C. corteziensis* after treatment ($P < 0.05$), but no significant difference in size within species was observed (Fig. 1B). Biomass was affected by species ($P < 0.05$) and by temperature ($P < 0.05$), with a significant decrease for *C. gigas* at 34 °C compared to the initial temperatures (Fig. 1C). Unfortunately, it was not possible to determine the sex of the oysters were without opening and sacrificing them. We employed 60 animals for each species, and could only distinguish their sex when final samples were taken. We sampled 10 oysters at 20 °C and 22 °C for each species, followed by 15 oysters at 28 °C, and the remaining individuals at 34 °C . We obtained an overall sex ratio of roughly 1:1.

3.2 Relative frequencies of oocytes

Normal previtellogenic, vitellogenic, and postvitellogenic oocytes of *C. gigas* and *C. corteziensis* are presented in Figures 2A and 2B, respectively. Hemocytes involved in the reabsorption of the gametes were observed in both *C. gigas* (Fig. 2C) and *C. corteziensis* (Fig. 2H).

Oocyte frequencies are shown in Figure 3. A significant difference between species was observed in oogonia frequencies ($P < 0.05$), with the highest proportion of oogonia observed in *C. corteziensis* (13% at 34 °C) compared to *C. gigas* (2.7% at 28 °C and 34 °C); no effect ($P > 0.05$) of temperature or the interaction was found (Fig. 3A). Previtellogenic oocytes were significantly affected by both factors and their interaction ($P > 0.05$, Fig. 3B). A greater frequency of previtellogenic oocytes was observed in *C. corteziensis* (20.1% at all temperatures) than in *C. gigas* (5.1% at all temperatures), and a greater number of previtellogenic oocytes was observed at 22 °C in *C. corteziensis* and at 20 °C in *C. gigas*. An effect of species was observed on the frequency of vitellogenic oocytes ($P < 0.05$, Fig. 3C). A higher proportion of vitellogenic oocytes was observed in *C. corteziensis* (27.3% at all temperatures) than in *C. gigas* (18.8% at all temperatures). The proportion of vitellogenic oocytes also declined with increasing temperature in both species ($P < 0.05$, Fig. 3C). Postvitellogenic oocytes were affected by species and temperature ($P < 0.05$, Fig. 3D), with a higher proportion of postvitellogenic oocytes in *C. gigas* (28.2% at all temperatures) than in *C. corteziensis* (11.3% at all temperatures), and late-developing oocytes decreased as temperature increased.

3.3 Oocyte condition and degeneration

284 Atretic oocytes, cells with structural degeneration, were observed mainly at the
285 vitellogenesis and postvitellogenesis stages for *C. gigas* (Fig. 2A) and *C. corteziensis* (Fig.
286 2B). Signs of oocyte degeneration were the loss of roundness of the cell and the nucleus
287 and folded cytoplasmic and nuclear membranes for *C. gigas* (Fig. 2C) and C. *corteziensis*
288 (Fig. 2D) and distention of the endoplasmic reticulum for *C. gigas* (Fig. 2E) and *C.*
289 *corteziensis* (Fig. 2F), and oocyte vacuolation was evident for both species (Figs. 2G, 4A,
290 and 4C for *C. gigas*, and Figs. 2H, 4B, and 4D for *C. corteziensis*). Oocyte autophagy was
291 found in both oyster species. The formation of autophagosomes was observed as small
292 round structures of different sizes without a nucleus and with an appearance and color
293 similar to the ooplasm of the oocytes in *C. gigas* (Figs. 4A and 4C) and *C. corteziensis*
294 (Figs. 4B and 4D). Large acidophilic and basophilic yolk granules and strong vacuolation
295 were observed in the ooplasm of atretic oocytes from both *C. gigas* and *C. corteziensis* after
296 thermal stress.
297 Vacuolated oocytes increased ($r = 0.5$; $P < 0.05$) with increasing temperature, from 0.85%
298 at 20 °C to 8.7% at 34 °C, with no differences found between species (Fig. 5A). Oocyte
299 atresia was significantly affected by species ($P < 0.05$, Fig. 5B), with the highest values in
300 *C. gigas* (11.7%) compared to *C. corteziensis* (6.4%). The frequency of cells with distended
301 endoplasmic reticulum increased directly proportionally to increasing temperature ($r = 0.4$;
302 $P < 0.05$), from 0.8% at 20 °C to 8.2% at 34 °C, without significant differences between
303 species (Fig. 5C). Degenerated oocytes (Fig. 5D) are expressed as the sum of all oocytes
304 that showed the signs of structural degeneration mentioned above, and they were
305 significantly higher in *C. gigas* (20.8%) than in *C. corteziensis* (12.5%, $P < 0.05$, Fig. 5D).
306 Temperature also affected degenerated oocytes, with significantly higher occurrences at

307 higher temperatures ($P < 0.05$, Fig. 5D). The autophagosome proportion increased as the
308 temperature rose ($P < 0.05$, Fig. 5E) from 20 °C (0.9%) to 34 °C (6.1%).
309
310 **3.4. Oocyte index (OI) and hemocyte index (HI)**
311 The area occupied by oocytes, expressed as the oocyte index (OI), was significantly
312 affected only by species ($P < 0.05$), with higher values in *C. gigas* (61.7 ± 4.34%) than in
313 *C. corteziensis* (35.6 ± 3.93%) (Fig. 7A). The hemocyte index (HI) was affected only by
314 temperature, which significantly increased from 2.63% at control temperatures of 20 °C
315 and 1.76% at 22 °C to 11.94% at 34 °C ($P < 0.05$, Fig. 7B). A direct and significant
316 relationship ($r = 0.5$ $P < 0.05$) was observed between thermal stress and hemocyte
317 infiltration in the gonads of both oyster species.
318
319 **3.5. Carbohydrates and lipids in gonads**
320 Neutral carbohydrates, mainly glycogen and glycoconjugates, were identified as
321 magenta-pink patches within the oocytes and in the surrounding vesicular connective
322 tissue in female gonads from both oyster species. As shown in Figures 6A and 6B,
323 carbohydrates stained intensely in the vesicular connective tissue, one of the main energy
324 storage tissues in oysters.
325 The lipid content found in female gonads consisted of neutral lipids (triglycerides) stained
326 in black-bluish hues and polar lipids (phospholipids) stained in gray blurs. The oocytes
327 had a higher triglyceride content than the oysters exposed to a higher temperature (34 °C),
328 while neutral lipid storage was not observed in vesicular connective tissue (Fig. 6C and
329 6D).

330 The carbohydrate content (carbohydrate index, %) was significantly affected by the
331 species, temperature, and interaction of the factors (Fig. 7C). In *C. gigas*, the carbohydrate
332 index decreased steadily and significantly from 51.74 ± 2.27% at 20 °C to 22.29 ± 2.76%
333 at 34 °C. In *C. corteziensis,* carbohydrates were significantly higher at 24 °C and 28 °C
334 (above 70%) but significantly decreased to 33.64 ± 6.44% at 34 °C ($P < 0.05$). The values
335 at 34 °C were similar for both species. An inverse relationship between the concentration
336 of carbohydrates stored in gonadal tissue and oocyte degeneration was observed, and this
337 energetic depletion was stronger in *C. gigas* ($r = -0.53$; $P < 0.05$) than in *C. corteziensis*
338 ($r = -0.49$; $P < 0.05$).
339 The lipid index steadily decreased ($r = -0.5$; $P < 0.05$) during the experiment from above
340 50% at 20 °C and 22 °C to values of approximately 30% at 28 °C and 34 °C in relation
341 to the temperature factor ($P < 0.05$), but no difference was found between species (Fig.
342 7D).
343
344 **3.6. Lipid peroxidation and lipofuscins**
345 Lipid peroxidation levels (TBARS) were affected by both factors (Species and
346 Temperature) and their interaction (Fig. 11A), with significantly higher levels in *C. gigas* at
347 28 °C (3,556 ± 626 nmol mg^{-1} protein) (Fig. 11A).
348 Lipofuscins stained with a lipophilic dye were identified as reddish granules in female
349 gonads of *C. gigas* (Fig. 8A) and *C. corteziensis* (Fig. 8C). Lipofusins appeared after the
350 reabsorption of degenerated oocytes. In Figures 8C and 8D, evidence of dense lipofuscin
351 granules inside brown cells from the two species is shown.
352 Both species and temperature had a significant effect on lipofuscin coverage area, with
353 higher values in *C. gigas* (7,400.16 μm^2 total) than in *C. corteziensis* (1,201.62 μm^2 total).

354 Lipofusin accumulation began at 28 °C, then a sudden increase ($P < 0.05$) at 34 °C was
355 found for *C. gigas*, and a slight but significant increase at the same temperature was
356 observed for *C. corteziensis* (Fig. 11B). A significant relationship ($r = 0.62$) between
357 increasing temperature and the accumulation of lipofuscins was found in the gonads of both
358 oysters.
359
360 **3.7. Heat shock protein (*Hsp*70) in gonads**
361 The detection of the *Hsp70* transcript in ovarian tissues from *C. gigas* and *C. corteziensis*
362 was performed using *in situ* hybridization (ISH) (Fig. 9). The signal intensity of the
363 coupling between the mRNA and labeled cDNA was assessed as the coverage area by
364 digital image analysis. The staining of *Hsp70* mRNA in the ovaries of both oyster species
365 was lowest ($P < 0.05$) at 20 °C (the control) and 22 °C, with no significant differences
366 between species found ($P > 0.05$) at these two temperatures. Transcript detection peaked to
367 its highest levels ($P < 0.05$) in both oyster species at 28 °C; at this temperature, *Hsp70*
368 mRNA detection levels were higher in the gonad of *C. corteziensis* (25,989 ± 1,555 μm^2)
369 than in *C. gigas* (8,803 ± 373 μm^2) ($P < 0.05$). The *Hsp70* transcript signal detection values
370 decreased significantly at 34 °C to the levels found at 22 °C for both species (Fig. 11C).
371
372 **3.8. Cell apoptosis**
373 Apoptotic hemocytes were observed both inside (Fig. 10A) and outside degenerating
374 oocytes, mainly phagocytic atretic oocytes in the two oysters (Fig. 10B and D). Oocytes
375 were observed breaking into apoptotic bodies, which are small vesicles that contain
376 fragments of nuclear material and cellular organelles, and part of the plasmatic membrane
377 (Fig. 10F).

The fluorescent signal of apoptotic cells was evaluated by digital image analysis and expressed as the hemocyte apoptosis index (Fig. 11D). Significant differences were obtained in the hemocyte apoptosis index for the species ($P < 0.05$) and temperature factor ($P < 0.05$) but not for the interaction. Hemocyte apoptosis increased with temperature ($r = 0.93$; $P < 0.05$) from less than 1% at 20 °C and 22 °C, regardless of species, until reaching the highest levels (above 60%) at 34 °C ($P < 0.05$). Both species had more hemocyte apoptosis at 28 °C, but it only reached a significant difference ($P < 0.05$) compared to 22 °C in *C. corteziensis* (19.2 ± 5.2%). At 34 °C, apoptosis significantly ($P < 0.05$) peaked at 64.9 ± 4.9% for *C. gigas* and 89.7 ± 2.7% for *C. corteziensis*.

3. DISCUSSION

The subtropical oyster *C. corteziensis* exhibits rapid growth and high gametogenic activity in waters at temperatures between 22 °C and 33 °C (Rodríguez-Jaramillo et al., 2008; Hurtado et al., 2012; Rodríguez-Jaramillo et al., 2017), in contrast to *C. gigas*, which is commonly grown in temperate zones where water does not increase above 22 °C (Cotter et al., 2010; Wendling et al., 2013). However, *C. gigas* has been introduced by several countries into warm waters that are frequently above 24 °C. Here, as expected, we found a significant decrease in survival for *C. gigas* when temperatures rose to 28 °C, and it decreased further at 34 °C, while in *C. corteziensis,* survival only decreased significantly at 34 °C (Fig. 1). Shells of *C. gigas* were larger than those of *C. corteziensis,* and this was of course not affected by temperature in a relatively short bioassay, but biomass was significantly decreased in *C. gigas* at 34 °C. Biomass loss could be a consequence of decreased food ingestion in oysters exposed to thermal stress, as suggested by Ren et al. (2000), with a lower microalgae clearance rate of *C. gigas* at

402 temperatures above 25 °C. Another possibility is biomass loss as a consequence of
403 forced spawning of immature oocytes in response to stress or reabsorption of the gonad
404 to face stress. We wanted to understand if there were differential mechanisms at tissue
405 levels that are put forward in *C. corteziensis* that enable it to withstand higher
406 temperatures and are lacking in *C. gigas*, and that eventually produce tissue
407 degeneration to a degree that is no longer compatible with life.
408 It has previously been proposed that temperature can accelerate gonad development and
409 affect the energetic budget in *C. gigas* and eventually promote energetic exhaustion,
410 gamete degeneration and high mortality (Berthelin et al., 2000; Fabioux et al., 2005;
411 Samain et al., 2007; Huvet et al., 2010). Several studies reported a direct correlation
412 between summer mortality events and reproductive effort in *C. gigas* (Berthelin et al.,
413 2000; Delaporte et al., 2007; Samain et al., 2007; Cotter et al., 2010; Huvet et al., 2010).
414 Here, we found that the oocyte index (Fig. 7) was higher in *C. gigas*, a result of larger
415 postvitellogenic oocytes, while in *C. corteziensis,* almost no postvitellogenic oocytes
416 were found at 34 °C (Fig. 3). *C. gigas* matures slowly during cold months and spawns as
417 temperature increases in summer (Delaporte et al., 2007; Samain et al., 2007). Under
418 natural conditions in the Gulf of California, *C. corteziensis* displays an opportunistic
419 reproductive strategy with continuous gametogenesis and partial spawning throughout
420 the year (Chávez-Villalba et al., 2007; Rodríguez-Jaramillo et al., 2008; Hurtado et al.,
421 2012). *C. gigas*, which is more susceptible to summer mortality, invests more energy in
422 reproduction (Delaporte et al., 2007; Huvet et al., 2010). Partial spawners recruit fewer
423 oocytes per spawn, using up fewer biochemical reserves to mature oocytes and investing
424 less energy in reproduction per spawn, thus leaving reserves that can be canalized to face
425 thermal stress. A higher reproductive effort in *C. gigas* as temperature increased was

426 coupled to lower carbohydrate content, suggesting a greater energy depletion in *C. gigas*
427 at higher temperatures. Carbohydrates are a major energy reserve in bivalves, and they
428 are oxidized to produce energy. *C. gigas*, which is less tolerant to summer mortality, had
429 more reactive oxygen species (ROS) production (Delaporte et al., 2007; Lambert et al.,
430 2007), and Delaporte et al. (2007) concluded that increased metabolism during maturation
431 *per se* could be considered a stress. Here, we found that *C. gigas* was more mature and
432 had significantly more TBARS, an indirect method of measuring ROS, at 28 °C than *C.*
433 *corteziensis* at the same temperature (Fig. 11). Maturation and temperature are two stress
434 factors that increase ROS; Rahman et al. (2019) also reported an increase in ROS
435 production in *C. gigas* as the temperature increased from 20 to 25 °C. Among other
436 factors, increased ROS production can upregulate the expression of heat shock proteins
437 (Landis et al., 2021), and a larger expression of heat shock proteins has been reported in
438 *C. gigas*, which is more tolerant to thermal stress, than in susceptible *C. gigas* (Lang et
439 al. 2009). Heat shock protein expression increased in mature stages in *C. gigas* compared
440 to resting gonads and then decreased after spawning, while levels in other tissues were
441 relatively stable (Meistertzheim et al., 2009), in accordance with increased metabolism
442 as a result of maturation producing stress. Here, we found that *Hsp*70 in gonads was
443 significantly higher at 28 °C in both species, in accordance with increased metabolism
444 and maturation. However, in *C. corteziensis,* expression was higher than in *C. gigas*, in
445 accordance with a higher capacity to neutralize stress in the former. Oxidized products
446 derived from oxidative damage accumulate in lysosomes, producing lipofuscins (Keller
447 et al., 2004). The results from this study show that *C. gigas* accumulated the highest
448 amounts of lipofuscins in the gonads as temperature increased, up to 7-fold higher at
449 28 °C and 20-fold higher at 34 °C than at 20–22 °C. In contrast, in *C. corteziensis*

lipofuscin levels were 2-fold higher at 34 °C than at 20 °C (Fig. 11B). Some studies have shown that excessive oxidative stress and lipofuscin accumulation may compromise the integrity of tissues and induce autophagy (Moore, 2008) and apoptosis (Matés et al., 2008; Sokolova, 2009; Zhang et al., 2011).

Another strategy to reduce reproductive effort in oysters with maturing gonads is to reabsorb oocytes or eject immature oocytes as inviable spawn. Oocytes degenerate as a strategy to recycle the energy reserves used to mature oocytes and channel them to other tissues to cope with periods of stress and energy depletion (Beninger et al., 2017). In the tropical oyster *C. gasar*, gametes are not expelled and are recycled in the digestive system (Diadhiou et al., 2019). Here, we found that degenerated oocytes significantly increased at higher temperatures in both species (Fig. 5D). Degenerated oocytes are no longer viable and are reabsorbed by several possible mechanisms, one of which is autophagy. Oocyte autophagy was found in both oyster species, with a significant increase at higher temperatures (Fig. 5E). Autophagy consists of degrading and recycling proteins and organelles from the cells through their inclusion into double-membrane vesicles called autophagosomes or autolysosomes, which leads to the degradation of the enclosed cytoplasmic components by lysosomal enzymes, as has been described in hemocytes of *C. gigas* (Picot et al., 2019). Starvation is the first trigger of autophagy and can be observed in several tissues of *C. gigas*, including gonads, using mRNA transcripts (Han et al., 2019; Picot et al., 2019), but it can also be induced by metabolic stress, drug treatment, radiation damage, and oxidative damage (Eisenberg-Lerner et al., 2009). Perturbation of autophagy has been associated with several diseases in *C. gigas* tissues, indicating that this process is involved in the maintenance of cellular homeostasis (Moreau et al., 2015). During reproduction, Kalachev et al. (2019) found more autophagic

474 vesicles in the cytoplasm of cells in the gonads of *C. gigas* in the active gametogenesis
475 stage than in the resting stage, indicating that it is probably a cyclic process associated
476 with gonad cleansing, used to save some of the energy previously invested into gonad
477 development. This would allow partial spawn to remove residual oocytes and their
478 biochemical reserves as a mechanism to reabsorb the gonads and the nutrients stored to
479 fuel gametogenesis.
480 Autophagy has a complex interplay with apoptosis. In some cellular settings, it can serve
481 as a cell survival pathway, suppressing apoptosis, and in others, it can lead to death itself,
482 either in collaboration with apoptosis or as a back-up mechanism when the former is
483 defective (Eisenberg-Lerner et al., 2009). Direct relationships have been found between
484 thermal stress and the apoptosis rate of all hemocyte types in *C. gigas* (Gagnaire et al.,
485 2006; Zhang et al., 2011). It has been suggested that temperatures close to 29 °C trigger
486 the expression of genes related to the apoptotic process and cell death and the
487 upregulation of genes related to autophagy (Delisle et al., 2020). We observed a higher
488 apoptotic index at higher temperatures, particularly for *C. corteziensis* at 28 °C and 34 °C
489 and for *C. gigas* at 34 °C. Higher apoptotic cell levels have been associated with a better
490 immune response in oyster species, as they remove damaged, senescent, and infected cells
491 (Terahara & Takahashi, 2008). Hemocyte apoptosis can represent the ultimate defense
492 response when the immune system is unable to clear the products of gamete degeneration
493 in a failed attempt of gonad maturation under stressful conditions (Sokolova, 2009; Kiss,
494 2010). Quickly induced atresia of oocytes with the concomitant increase in apoptotic
495 hemocytes might be a mechanism in partial spawners that could increase tolerance to
496 summer mortality.

497 The results from this study support the theory that summer mortality is a multifactorial
498 phenomenon (Samain et al., 2007; Fleury et al., 2020), where gonad formation and
499 physiological status are suspected to play key roles in the outcome of the interaction with
500 their environment. Profound ecophysiological differences exist between tropical and
501 subtropical Ostreidae of the American Pacific, mainly those related to the gametogenic
502 development of their populations in a latitudinal form (Rodríguez-Jaramillo et al., 2017).
503 Our results from this study suggest that the overall physiological status of oysters,
504 particularly during simultaneous gamete production and thermal stress, plays a significant
505 role in the massive mortalities of susceptible species such as *C. gigas* and corroborates
506 the ideas stated by Samain et al. (2007) and Huvet et al. (2010), where summer mortalities
507 of this species during warmer months may be due to metabolic disturbances in oysters
508 associated with their reproductive effort under conditions of thermal stress. Nonetheless,
509 transcriptomic and proteomic approaches to compare the responses between *C. gigas* and
510 *C. corteziensis* could confirm these suggestions. Additionally, a comparison with males,
511 which should be more tolerant to increases in temperature because energy output for
512 female gonad development is higher, could indicate more clearly what mechanisms are
513 triggered by sex.
514
515 **Conclusions.**
516 This study provides evidence of differences between the introduced temperate *C. gigas* and
517 the native tropical *C. corteziensis* in response to increasing temperatures during
518 reproduction. The Pacific Oyster displayed the highest rates of mortality, biomass losses,
519 oocyte degeneration, and depletion of energy reserves during gametogenesis and higher
520 expression of the *Hsp*70 transcript. It is possible that these differences have an evolutionary

and adaptive basis, which results in distinct capabilities to face high temperatures in the summer. Summer mortalities can trigger worldwide economic losses in oyster aquaculture and threaten natural beds of wild populations. The information provided by this study could contribute to improving genetic selection programs of oyster families tolerant to elevated temperatures and to establishing oyster aquaculture strategies that are less susceptible to the changing global environment.

Acknowledgments.

This study was conducted with support from SEP-CONACYT 286252, awarded to E. Palacios. We are grateful to Eulalia Meza Chávez, Neftaly Gutierrez, Orlando Lugo, Fabiola Arcos and Cesar Ruíz for their assistance during the bioassay and sample analysis.

Conflict of interest

The authors declare no conflicts of interest.

Data availability statement

The data that support the findings of this study are available from the corresponding author upon reasonable request.

Ethics statements

The adult oysters (*C. gigas* and *C. corteziensis*) were transported and handled according to CIBNOR Internal Committee for the Care and Use of Laboratory Animals (CICUAL), and the number of sampled organisms contemplated "the rule of maximizing information

544 published and minimizing unnecessary studies". In this sense, 140 oysters were considered
545 the minimum number of organisms needed for this experiment.
546
547
548 **References.**

549 Abele, D., Philipp, E., Gonzalez, P., Puntarulo, S., 2007. Marine invertebrate mitochondria
550 and oxidative stress. Front. Biosci. 12, 933–946. https://doi.org/10.2741/2115
551 Beninger, P.G., 2017. Caveat observator: the many faces of pre-spawning atresia in marine
552 bivalve reproductive cycles. Mar. Biol. 164, 1-12.
553 https://link.springer.com/article/10.1007/s00227-017-3194-x
554 Berthelin, C., Kellner, K., Mathieu, M., 2000. Storage metabolism in the Pacific oyster
555 (*Crassostrea gigas*) in relation to summer mortalities and reproductive cycle (West
556 Coast of France). Comp. Biochem. Physiol. 125B, 359–369. https://doi:10.1016/s0305-
557 0491(99)00187-x
558 Brunk, U.T., Terman, A., 2002. Lipofuscin: Mechanisms of age-related accumulation and
559 influence on cell function. Free Radical Bio. Med. 33, 611–619.
560 https://doi:10.1016/S0891-5849(02)00959-0
561 Boullot, F., Castrec, J., Bidault, A., Dantas, N., Payton, L., Perrigault, M., Tran, D., Amzil,
562 Z., Boudry, P., Soudant, P., Hégaret, H., Fabioux, C., 2017. Molecular characterization
563 of voltage-gated sodium channels and their relations with paralytic shellfish toxin
564 bioaccumulation in the pacific oyster *Crassostrea gigas*. Mar. Drugs. 15(1), 21.
565 https://doi.org/10.3390/md15010021
566 Castillo-Durán, A., Chávez-Villalva, J., Arreola-Lizarraga, A., Barraza-Guajardo, R., 2010.
567 Comparative growth, condition, and survival of juvenile *Crassostrea gigas* and *C.*

568 *corteziensis* oysters cultivated in summer and winter. Cienc. Mar. 36, 29-
569 https://doi:10.7773/cm.v36i1.1623
570 Chávez-Villalba, J., Villelas-Ávila, R., Cáceres-Martínez, C., 2007. Reproduction,
571 condition and mortality of the Pacific oyster *Crassostrea gigas* (Thunberg) in Sonora,
572 México. Aquacult. Res. 38, 268–278.https://doi:10.1111/j.1365-2109.2007.01662.x
573 Cotter, E., Malham, S. K., O'Keeffe, S., Lynch, S. A., Latchford, J. W., King, J. W.,
574 Beaumont, A. R., Culloty, S. C., 2010. Summer mortality of the Pacific oyster,
575 *Crassostrea gigas*, in the Irish Sea: The influence of growth, biochemistry and
576 gametogenesis. Aquaculture 303, 8-21. https://doi:10.1016/j.aquaculture.2010.02.030
577 Diadhiou, H. D., Ndour, I., Sarr, S. M., Djimera, A., 2019. Oocyte atresia in the Mangrove
578 oyster, *Crassostrea gasar* (Dautzenberg 1891), (Bivalvia Ostreidae) in tropical
579 environment. Int. J. Biol. Chem. Sci. 13, 1082–1093.
580 Delaporte, M., Soudant, P., Lambert, C., Jegaden, M., Moal, J., Pouvreau, S., Dégremont,
581 L., Boudry, P., Samain, J.F., 2007. Characterisation of physiological and
582 immunological differences between Pacific oysters (*Crassostrea gigas*) genetically
583 selected for high or low survival to summer mortalities and fed different rations under
584 controlled conditions. J. Exp. Mar. Biol. Ecol. 353, 353, 45–57.
585 https://doi.org/10.1016/j.jembe.2007.09.003
586 Delisle, L., Pauletto, M., Vidal-Dupiol, J., Petton, B., Bargelloni, L., Montagnani, C.,
587 Pernet, F., Corporeau, C., Fleury, E., 2020. High temperature induces transcriptomic
588 changes in *Crassostrea gigas* that hinders progress of Ostreid herpesvirus (OsHV-1)
589 and promotes survival. J. Exp. Biol. Jeb226233 https://doi.org/10.1242/jeb.226233
590 Dutertre, M., Beninger, P. G., Barille, L., Papin, M., Rosa, P., Barille, A., Haure, J., 2009.
591 Temperature and seston quantity and quality effects on field reproduction of farmed

592 oysters, *Crassostrea gigas*, in Bourgneuf Bay, France. Aquat. Living Res. 22, 319-329.
593 https://doi.org/10.1051/alr/2009042
594 Eisenberg-Lerner, A., Bialik, S., Simon, H.-U., Kimchi, A., 2009. Life and death partners:
595 apoptosis, autophagy and the cross-talks between them. Cell Death Differ. 16, 966-75.
596 https://doi.org/10.1038/cdd.2009.33
597 Fabioux, C., Huvet, A., Le Souchu, P., Le Pennec, M., Pouvreau, S., 2005. Temperature
598 and photoperiod drive *Crassostrea gigas* reproductive internal clock. Aquaculture, 250,
599 458–470. https://doi:10.1016/j.aquaculture.2005.02.038
600 Fleury, E., Barbier, P., Petton, B., Normand, J., Thomas, Y., Pouvreau, S., Daigle, G.,
601 Pernet, F., 2020. Latitudinal drivers of oyster mortality: deciphering host, pathogen and
602 environmental risk factors. Sci. Rep. 10, 7264 https://www.nature.com/articles/s41598-
603 020-64086-1.pdf
604 Gagnaire, B., Frouin, H., Moreau, K., Thomas-Guyon, H., Renault, T., 2006. Effects of
605 temperature and salinity on haemocyte activities of the pacific oyster, *Crassostrea*
606 *gigas* (Thunberg). Fish Shellfish Immun. 20, 536–547.
607 https://doi.org/10.1016/j.fsi.2005.07.003
608 Guerra, C., Zenteno-Savín, T., Maeda-Martínez, A. N., Philipp, E. E. R., Abele, D., 2012.
609 Changes in oxidative stress parameters in relation to age, growth and reproduction in
610 the short-lived Catarina scallop *Argopecten ventricosus* reared in its natural
611 environment. Comp. Biochem. Physiol. 162A, 421–430.
612 https://doi.org/10.1016/j.cbpa.2012.04.018
613 Han, Z., Wang, W., Lv, X., Zong, Y., Liu, S., Liu, Z., Wang,L., Song, L., 2019. ATG10
614 (autophagy-related 10) regulates the formation of autophagosome in the anti-virus

615 immune response of Pacific oyster (*Crassostrea gigas*). Fish Shellfish Immun. 91,
616 325–332. https://doi.org/10.1016/j.fsi.2019.05.027
617 Höhn, A., Jung, T., Grimm, S., Catalgol, B., Weber, D., Grune, T., 2011. Lipofuscin
618 inhibits the proteasome by binding to surface motifs. Free Radical Biol. Med. 50, 585–
619 591. https://doi.org/10.1016/j.freeradbiomed.2010.12.011
620 Hurtado, M.A., Racotta, I.S., Arcos, F., Morales-Bojórquez, E., Moal, J., Soudant, P.,
621 Palacios, E., 2012. Seasonal variations of biochemical, pigment, fatty acid, and sterol
622 compositions in female *Crassostrea corteziensis* oysters in relation to the reproductive
623 cycle. Comp. Biochem. Physiol. 163B, 172-183.
624 https://doi.org/10.1016/j.cbpb.2012.05.011
625 Hurtado-Oliva, M.A., Gómez-Hernández, S.J., Gutiérrez-Rivera, J.N., Estrada, N., Piña-
626 Valdez, P., Nieves-Soto, M., Medina-Jasso, M. A., 2015. Gender Differences and
627 Short-Term Exposure to Mechanical, Thermic, and Mechanical—Thermic Stress
628 Conditions on Hemocyte Functional Characteristics and HSP70 Gene Expression in
629 Oyster *Crassostrea corteziensis* (Hertlein, 1951). J. Shellfish Res. 34, 849–859.
630 https://doi.org/10.2983/035.034.0314
631 Huvet, A., Normand, J., Fleury, E., Quillien, V., Fabioux, C., Boudry, P., 2010.
632 Reproductive effort of Pacific oysters: A trait associated with susceptibility to summer
633 mortality. Aquaculture. 304, 95-99. https://doi:10.1016/j.aquaculture.2010.03.022
634 Jackson, S.A., Uhlinger, K.R., Clegg, J.S., 2011. Duration of induced thermal tolerance and
635 tissue-specific expression of hsp/hsc70 in the eastern oyster, *Crassostrea virginica* and
636 the Pacific oyster, *Crassostrea gigas*. Aquaculture. 317, 168–174.
637 https://doi.org/10.1016/j.aquaculture.2011.04.004

638 Jung, T., Bader, N., Grune, T., 2007. Lipofuscin: Formation, distribution, and metabolic
639 consequences. Ann. N.Y. Acad. Sci. 1119, 97–111.
640 https://doi:10.1196/annals.1404.008
641 Kalachev, A. V., Yurchenko, V. O., 2019. Autophagy in nutrient storage cells of the Pacific
642 oyster, *Crassostrea gigas*. Tissue Cell. 61, 30–34.
643 https://doi.org/10.1016/j.tice.2019.08.007.
644 Keller, J.N., Dimayuga, E., Chen, Q., Thorpe, J., Gee, J., Ding, Q., 2004. Autophagy,
645 proteasomes, lipofuscin, and oxidative stress in the aging brain. Int. J. Biochem. Cell
646 Biol. 36, 2376–2391. https://doi:10.1016/j.biocel.2004.05.003
647 Kiss, T., 2010. Apoptosis and its functional significance in molluscs. Apoptosis, 15, 313–
648 21. https://doi:10.1007/s10495-009-0446-3
649 Lambert, C., Soudant, P., Dégremont, L., Delaporte, M., Moal, J., Jean, F., Huvet, A.,
650 Samain, J.F., 2007. Hemocyte characteristics in families of oysters, *Crassostrea gigas*,
651 selected for differential survival during summer and reared in three sites. Aquaculture,
652 270, 276–288. https://doi.org/10.1016/j.aquaculture.2007.03.016
653 Landis, G., Shen, J., Tower, J. 2012. Gene expression changes in response to aging
654 compared to heat stress, oxidative stress and ionizing radiation in *Drosophila*
655 *melanogaster*. Aging, 4, 768-789. https://doi:10.18632/aging.100499
656 Lang, R.P., Bayne, C.J., Camara, M.D., Cunningham, C., Jenny, M.J., Langdon, C.J., 2009.
657 Transcriptome profiling of selectively bred Pacific oyster *Crassostrea gigas* families
658 that differ in tolerance of heat shock. Mar. Biotechnol. 11, 650–68.
659 https://doi:10.1007/s10126-009-9181-6

660 Le Pennec, M., Beninger, P., Dorange, G., Paulet, Y., 1991. Trophic Sources and Pathways
661 to the Developing Gametes of *Pecten maximus* (Bivalvia: Pectinidae). J. Mar. Bio. Ass.
662 U.K. 71, 451-463. doi:10.1017/S0025315400051705
663 Matés, J.M., Segura, J.A., Alonso, F.J., Marquéz, J., 2008. Intracellular redox status and
664 oxidative stress: implications for cell proliferation, apoptosis, and carcinogenesis.
665 Arch. Toxicol. 82, 273–299. https://doi.org/10.1007/s00204-008-0304-z
666 Meistertzheim, A.L., Lejart, M., Le Goïc, N., Thébault M. T., 2009. Sex-, gametogenesis,
667 and tidal height-related differences in levels of HSP70 and metallothioneins in the
668 Pacific oyster *Crassostrea gigas*. Comp. Biochem. Physiol. 152A, 234-239.
669 https://www.sciencedirect.com/science/article/pii/S109564330801163X?via%3Dihub
670 Moore, M. N., 2008. Autophagy as a second level protective process in conferring
671 resistance to environmentally-induced oxidative stress. Autophagy. 4, 254–256.
672 https://doi.org/10.4161/auto.5528
673 Moreau, P., Moreau, K., Segarra, A., Tourbiez, D, Travers, M. A., Rubinsztein, D.C.,
674 Renault, T., 2015. Autophagy plays an important role in protecting Pacific oysters from
675 OsHV-1 and *Vibrio aestuarianus* infections. Autophagy. 11, 516-26.
676 https://www.tandfonline.com/doi/full/10.1080/15548627.2015.1017188
677 Picot, S., Morga, B., Faury, N., Chollet, B., Dégremont, L., Travers, M.A., Renault, T.,
678 Arzul, I., 2019. A study of autophagy in hemocytes of the Pacific oyster, *Crassostrea*
679 *gigas*. Autophagy, 15, 1801-1809. https://doi.org/10.1080/15548627.2019.1596490
680 Rahman, M. A., Henderson, S., Miller-Ezzy, P., Li, X. X., Qin, J. G., 2019. Immune
681 response to temperature stress in three bivalve species: Pacific oyster *Crassostrea*
682 *gigas*, Mediterranean mussel *Mytilus galloprovincialis* and mud cockle *Katelysia*

683 *rhytiphora*. Fish Shellfish Immunol. 86, 868–874.
684 https://doi:10.1016/j.fsi.2018.12.017.
685 Ren, J.S., Ross, A.H., Schiel, D.R., 2000. Functional descriptions of feeding and energetics
686 of the Pacific oyster *Crassostrea gigas* in New Zealand. Mar. Ecol. Prog. Ser. 208,
687 119-130. https://doi.org/10.3354/meps208119
688 Rodríguez-Jaramillo, C., Hurtado, M.A., Romero-Vivas, E., Ramírez, E., Manzano, M.,
689 Palacios, E., 2008. Gonadal development and histochemistry of the tropical oyster,
690 *Crassostrea corteziensis* (Hertlein, 1951) during an annual reproductive cycle. J.
691 Shellfish Res. 27, 1129–1141. https://doi.org/10.2983/0730-8000-27.5.1129.
692 Rodríguez-Jaramillo, C., Ibarra, A. M., Soudant, P., Palacios, E. 2017. Comparison of
693 quantitative gonad maturation scales in a temperate oyster (*Crassostrea gigas*) and a
694 sub-tropical oyster (*Crassostrea corteziensis*). Invertebr. Reprod. Dev. 61, 147–156.
695 https://doi:10.1080/07924259.2017.1315341
696 Samain, J. F., Dégremont, L., Soletchnik, P., Haure, J., Bédier, E., Ropert, M., Moala, J.,
697 Huvet, A., Bacca, H., Van Wormhoud, H., Delaporte, M., Costil, K., Pouvreau, S.,
698 Lambert, C., Boulo, V., Soudant, P., Nicolas, J.L., Le Roux, F., Renault, T., Gagnaire,
699 B., Geret, F., Boutet, I., Burgeot, T., Boudry, P., 2007. Genetically based resistance to
700 summer mortality in the Pacific oyster (*Crassostrea gigas*) and its relationship with
701 physiological, immunological characteristics and infection processes. Aquaculture,
702 268, 227–243. https://doi:10.1016/j.aquaculture.2007.04.044
703 Sokolova, I.M., 2009. Apoptosis in molluscan immune defense. Invertebr. Surv. J. 6, 49–
704 58. https://www.isj.unimore.it/index.php/ISJ/article/view/179
705 Soletchnik, P., Faury, N., Goulletquer, P., 2006. Seasonal changes in carbohydrate
706 metabolism and its relationship with summer mortality of Pacific oyster *Crassostrea*

gigas (Thunberg) in Marennes-Oléron bay (France). Aquaculture. 252, 328–338. https://doi.org/10.1016/j.aquaculture.2005.07.008

Terahara, K., Takahashi, K.G., 2008. Mechanisms and immunological roles of apoptosis in molluscs. Curr. Pharm. Design. 14, 131–137. https://doi.org/10.2174/138161208783378725

Terman, A., Brunk, U.T., 2004. Lipofuscin. Int. J. Biochem. Cell Biol. 36, 1400–1404. https://doi:10.1016/j.biocel.2003.08.009

Wendling, C. C., Wegner, K. M., 2013. Relative contribution of reproductive investment, thermal stress and Vibrio infection to summer mortality phenomena in Pacific oysters. Aquaculture. 412, 88–96. https://doi:10.1016/j.aquaculture.2013.07.009

Zar, J.H. 2010. Biostatistical Analysis. 5th Ed. Pearson, Westlake Village, CA, 251 pp. ISBN-13: 978-0130815422

Zhang, L., Li, L., Zhang, G., 2011. Gene discovery, comparative analysis and expression profile reveal the complexity of the Crassostrea gigas apoptosis system. Dev. Comp. Immunol. 35, 603–10. https://doi:10.1016/j.dci.2011.01.005

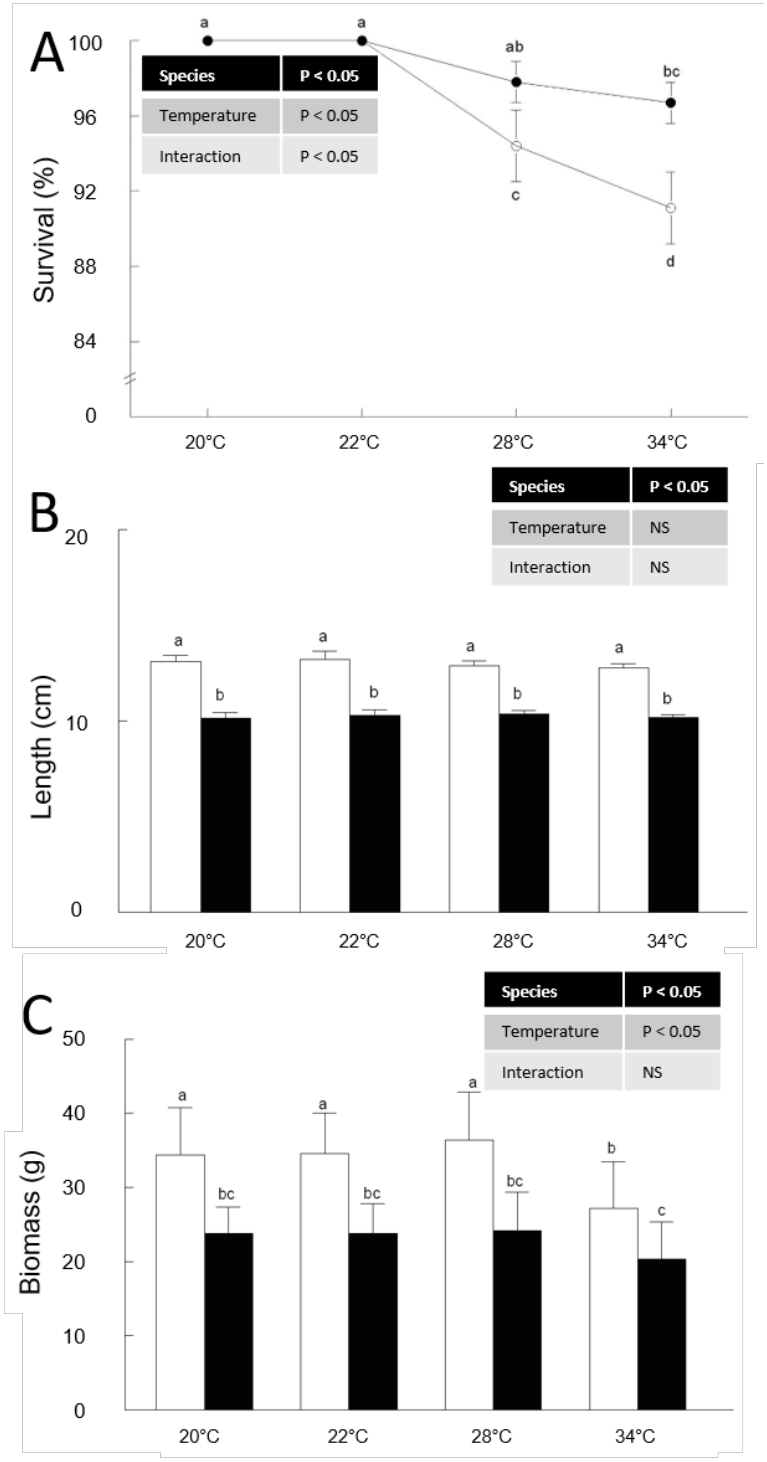

722

723 **Figure 1**. A) Survival rate; B) Length, and C) Biomass of *Crassostrea gigas* (n = 23; white
724 circles or bars) and *Crassostrea corteziensis* (n = 11; black circles or bars) exposed to a
725 controlled increase in temperature. The data (mean ± SE) were analyzed using the
726 temperature (4 levels) and species (two levels) as independent variables in a two-way
727 ANOVA. Different letters denote statistically significant differences after a multiple means
728 comparison Tukey-HSD test (significance at $P < 0.05$).

729

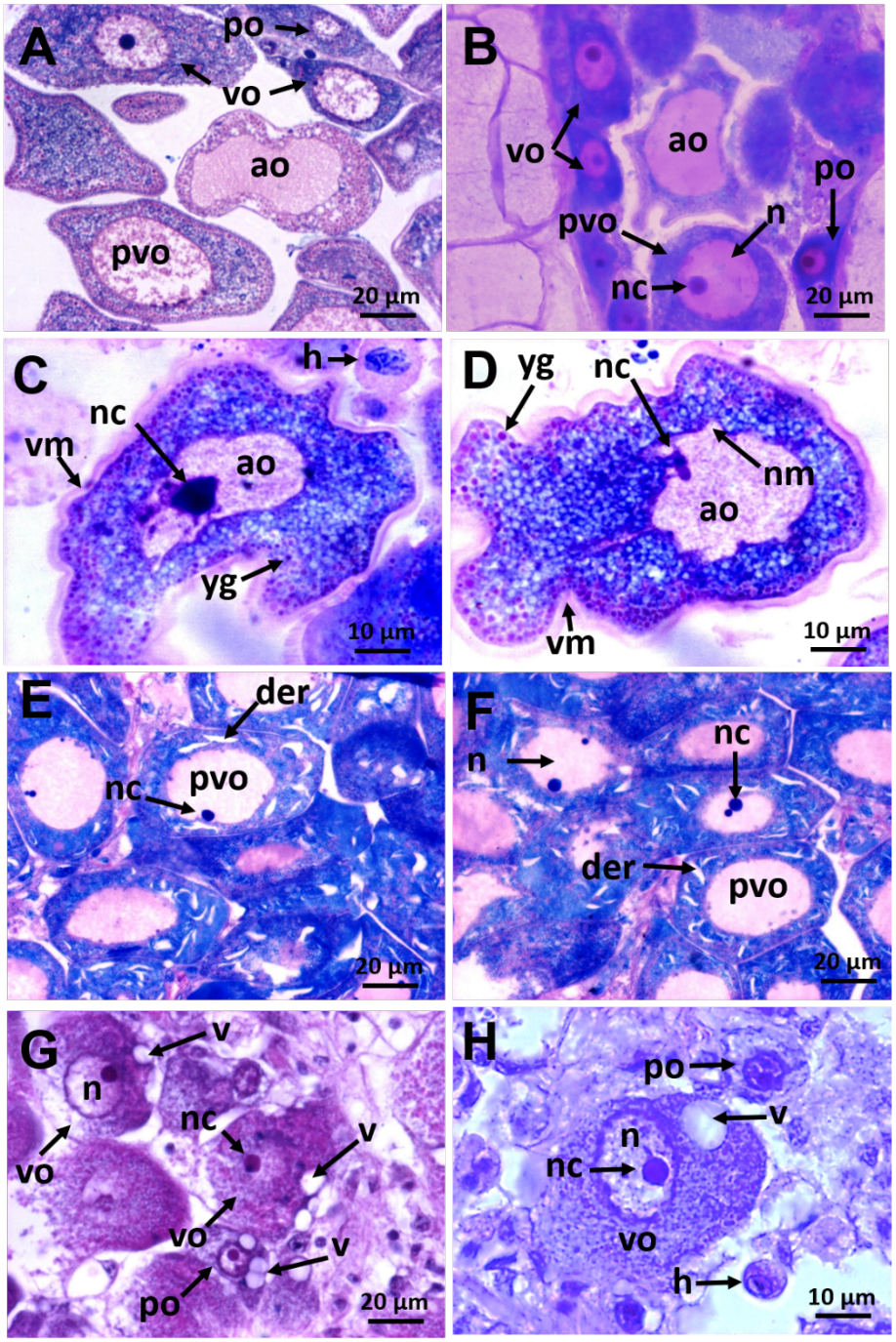

730

731 **Figure 2**. Microphotographs of histological sections of gonads of *Crassostrea gigas* A), C),
732 E, G) and *Crassostrea corteziensis* B), D), and F) exposed to a controlled increase in
733 temperature. H); po, previtellogenic oocytes; vo, vitellogenic oocytes; opv, postvitellogenic
734 oocytes; ao; atretic oocytes; n, nucleus; nc nucleolus; vm, vitelline membrane; yg, yolk
735 granules; nm, nuclear membrane; distended endoplasmic reticulum (der); v, vacuoles. A-F)
736 Resin sections (1 µm, Polychromium staining). G–H) Paraffin cuts (4 µm, hematoxylin and
737 eosin staining).

738

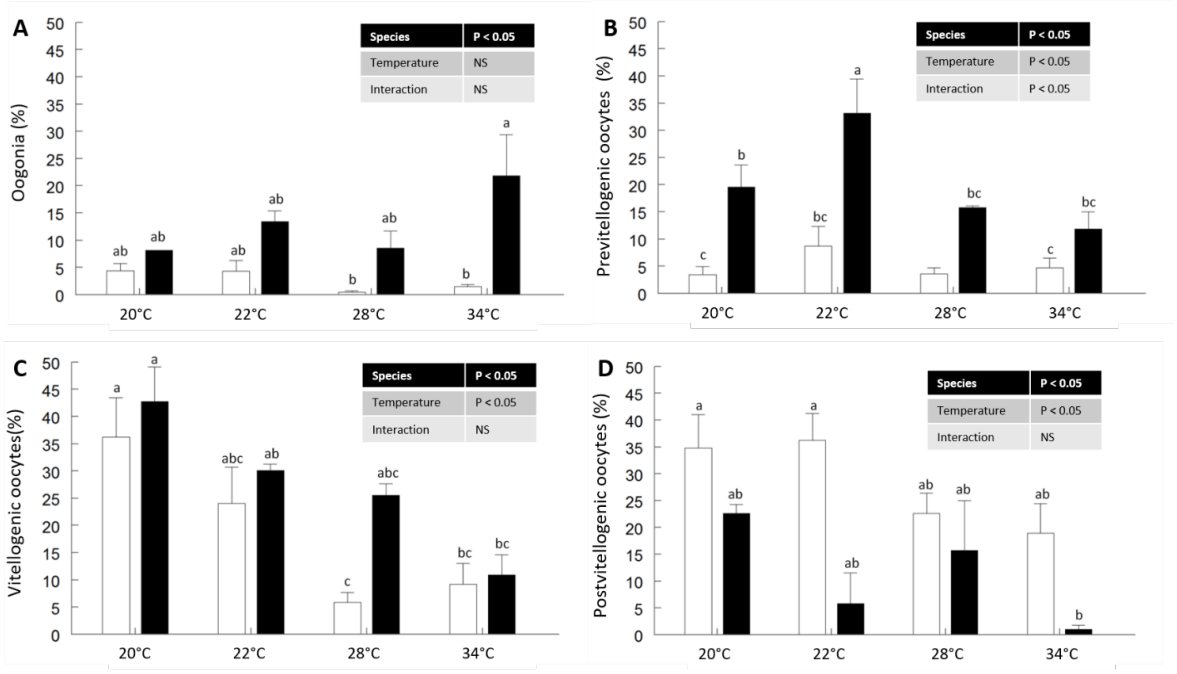

739

740 **Figure 3**. Relative frequencies of oocytes in female gonads of *Crassostrea gigas* (n = 23;
741 white bars) and *Crassostrea corteziensis* (n = 11; black bars) exposed to a controlled
742 increase in temperature. A) Oogonia; B) Previtellogenic oocytes; C) Vitellogenic oocytes;
743 D) Postvitellogenic oocytes. The data (mean ± SE) were analyzed using the temperature (4
744 levels) and species (two levels) as independent variables in a two-way ANOVA. Different
745 letters denote statistically significant differences after a multiple means comparison Tukey-
746 HSD test (significance at $P < 0.05$).

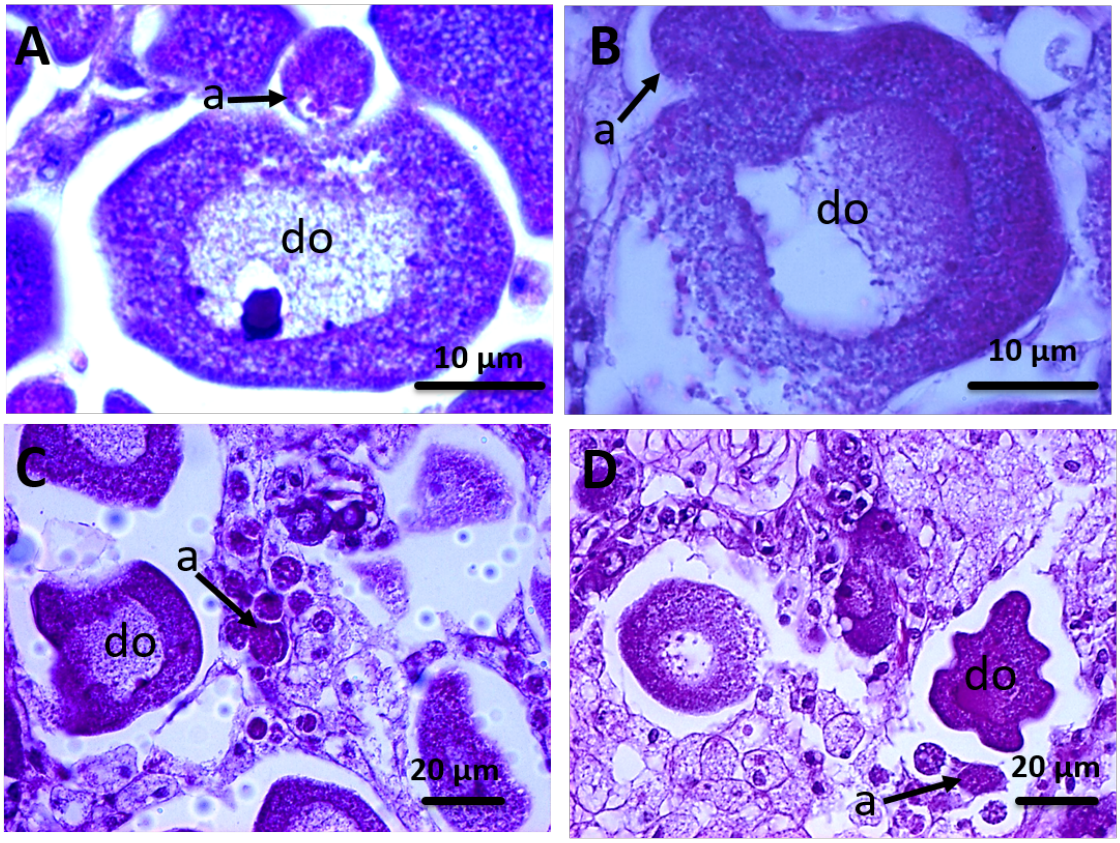

747
748 **Figure 4**. Microphotographs of histological sections of gonads from oysters exposed to a
749 controlled increase in temperature with oocytes in autophagy. A) and C) *Crassostrea gigas*;
750 B) and D) *Crassostrea corteziensis*; a, autophagosomes; do, degenerated oocyte. Paraffin
751 sections (4 µm, hematoxylin and eosin staining).

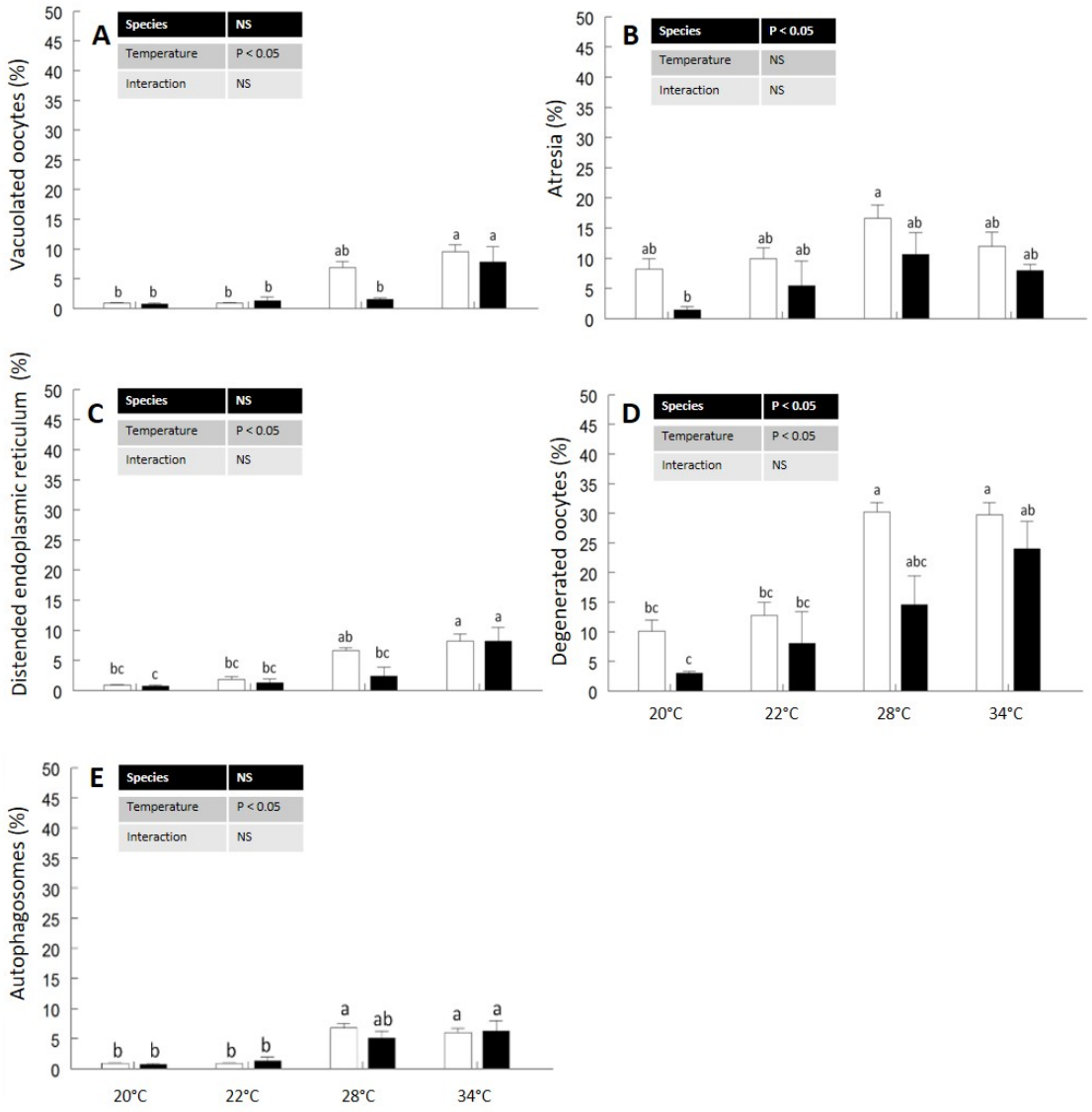

Figure 5. Relative frequency of degenerated oocytes and autophagosomes in *Crassostrea gigas* (n = 23; white bars) and *Crassostrea corteziensis* (n = 11; black bars) exposed to a controlled increasing temperature. A) Vacuolated oocytes; B) Atresia; C) Oocytes with distended endoplasmic reticulum; D) Degenerated oocytes; E) Autophagosomes. The data (mean ± SE) were analyzed using the temperature (4 levels) and species (two levels) as independent variables in a two-way ANOVA. Different letters denote statistically significant differences after a multiple means comparison Tukey-HSD test (significance at $P < 0.05$).

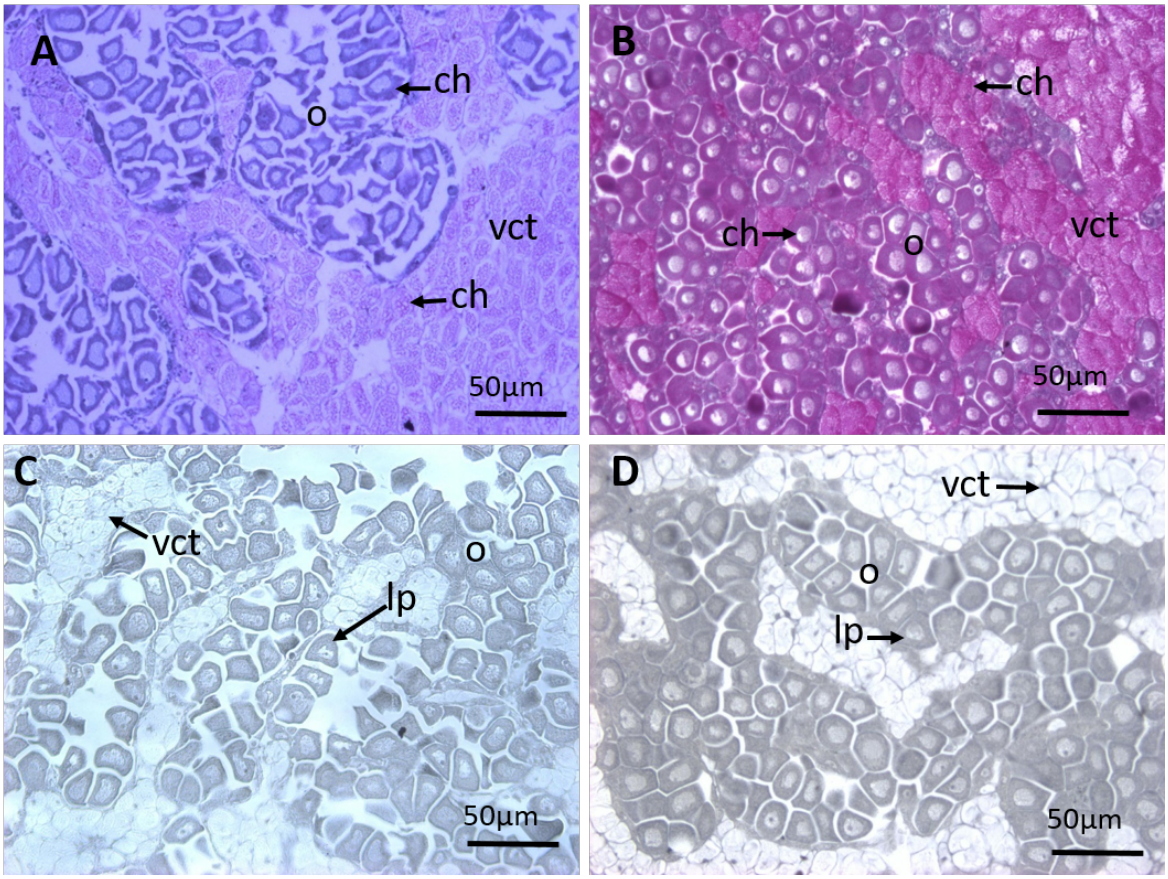

763

764 **Figure 6**. Microphotographs of energy substrates stored in female gonads of oysters exposed
765 to a controlled increase in temperature. A) Carbohydrates in *Crassostrea gigas*; B)
766 Carbohydrates in *Crassostrea corteziensis*; C) Lipids in *C. gigas*; D) Lipids in *C.*
767 *corteziensis*; ch, carbohydrates; lp, lipids; o, oocytes, vct, vesicular connective tissue.
768 Paraffin sections (4 µm); A) and B) PAS staining. C) and D) Sudan black staining.

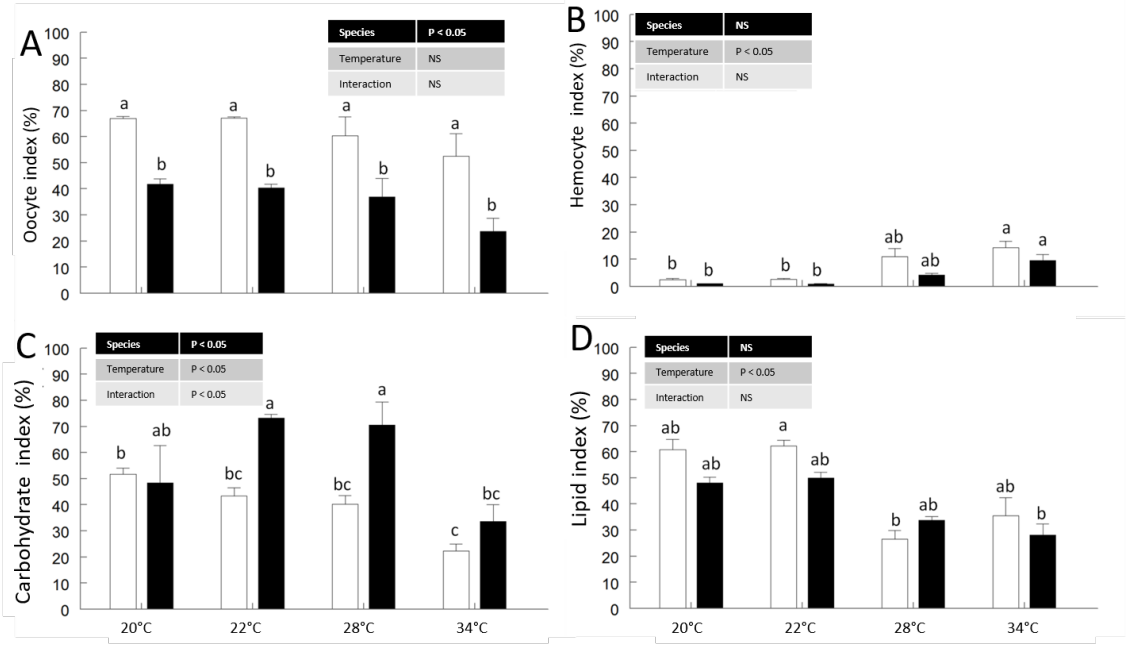

Figure 7. A) Oocyte index (OI); B) Hemocyte index (HI); C) Carbohydrate index; D) Lipid index in gonads of *Crassostrea gigas* (n = 23) white bars and *Crassostrea corteziensis* (n = 11) black bars exposed to a controlled increase in temperature. The data (mean ± SE) were analyzed using the temperature (4 levels) and species (two levels) as independent variables in a two-way ANOVA. Different letters denote statistically significant differences after a multiple means comparison Tukey-HSD test (significance at $P < 0.05$).

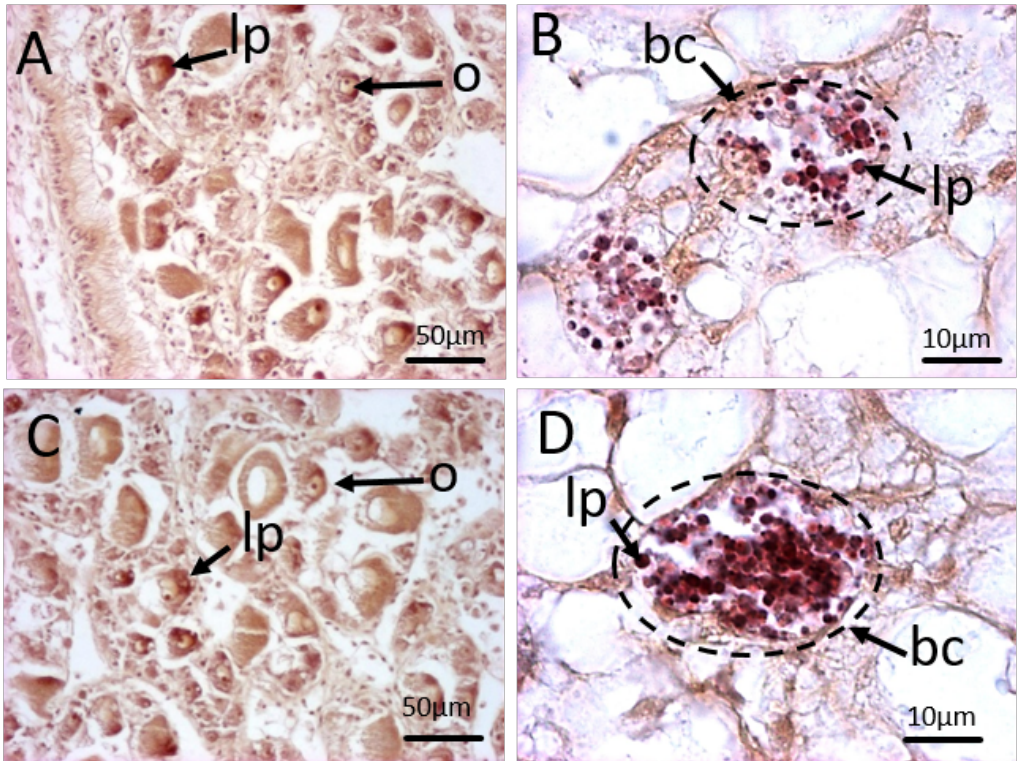

780
781
782 **Figure 8.** Microphotographs of lipofuscins in female gonads of A) *C. gigas*; B)
783 lipofuscins within brown cells of *Crassostrea gigas*; C) lipofuscins in female gonads of
784 *Crassostrea corteziensis*; D) lipofuscins within brown cells of *C. corteziensis* exposed to
785 a controlled increase in temperature; o, oocyte; lp, lipofuscins; bc, brown cell. Paraffin
786 sections (4 µm, Kinyoun Carbol Fuchsin staining).

787

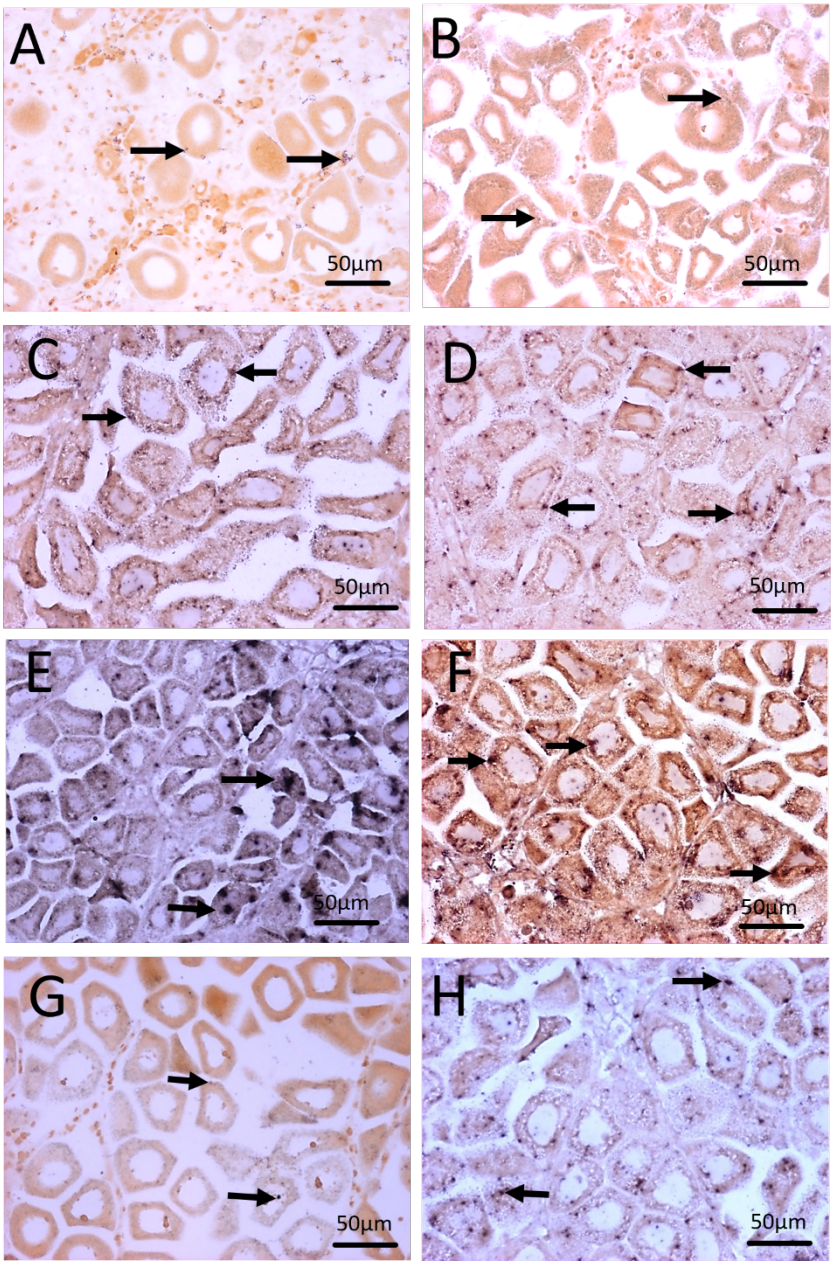

788
789
790 **Figure 9.** Localization of *Hsp70* transcript signal by ISH in ovaries from oysters exposed
791 to a controlled increasing temperature (arrows). Positive hybridization of *Hsp70* antisense
792 probe in oocytes A) *Crassostrea gigas* and B) *Crassostrea corteziensis* at 20 °C. C) *C*
793 *gigas* and D) *C. corteziensis* at 22 °C. E) *C. gigas* and F) *C. corteziensis* at 28 °C. G) *C.*
794 *gigas* and H) *C. corteziensis* at 34 °C. Paraffin sections (4 µm).

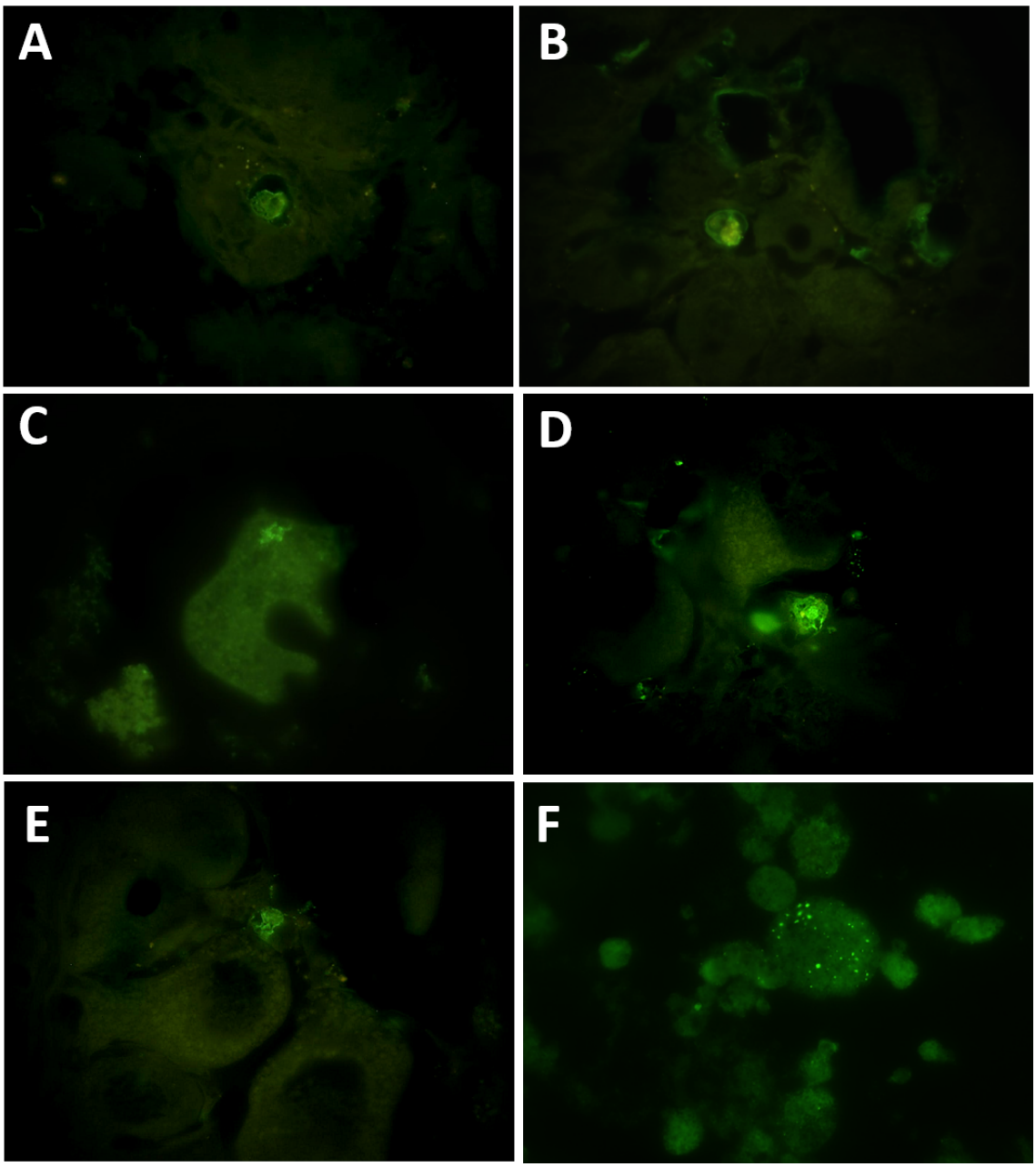

Figure 10. Microphotographs of apoptotic cells in gonads from oysters exposed to an experimental temperature of 34 °C. A) Hemocytes undergoing apoptosis within a *Crassostrea gigas* oocyte; B) Hemocytes undergoing apoptosis within a *Crassostrea corteziensis* oocyte; C) Apoptotic hemocyte into oocyte with fragmented DNA; D) Hemocytes undergoing apoptosis on one side of an atretic oocyte; E) Hemocytes undergoing apoptosis on one side of a degenerating oocyte; F) Apoptotic bodies in female gonads. Paraffin sections (4 µm, TUNEL technique).

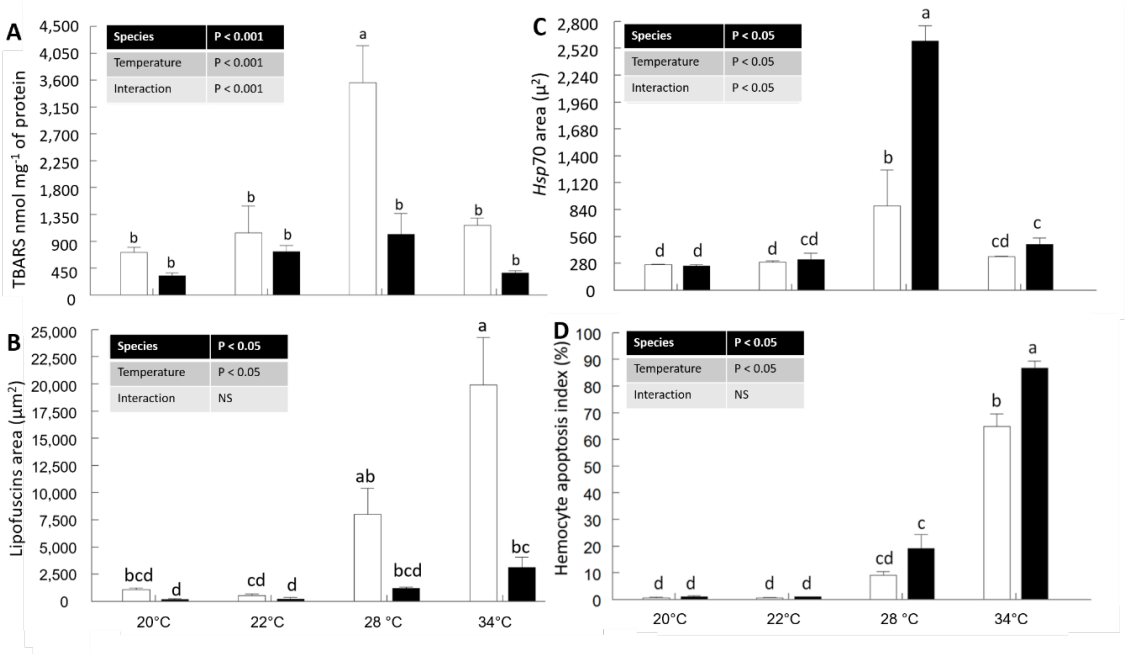

Figure 11. A) Peroxidized lipids TBARS; B) Lipofuscin coverage area; C) *Hsp70* transcript signal area (µm²); D) Hemocyte apoptosis index in gonads of *Crassostrea gigas* (n = 23; white bars) and *Crassostrea corteziensis* (n = 11; black bars) exposed to a controlled increase in temperature. The data (mean ± SE) were analyzed using the temperature (4 levels) and species (two levels) as independent variables in a two-way ANOVA. Different letters denote statistically significant differences after a multiple means comparison Tukey-HSD test (significance at $P < 0.05$).